Ocean-Atmosphere Water Flux and Evaporation

W. Timothy Liu and Xiaosu Xie
Jet Propulsion Laboratory
California Institute of Technology
MS 300-323, 4800 Oak Grove Dr.
Pasadena, CA 91109, U.S.A.
Email: w.t.liu@jpl.nasa.gov
Tel: 818-354-2394

Definition

The ocean-atmosphere water exchange is the difference between evaporation and precipitation at the surface of the ocean. Evaporation is the turbulent transport of water vapor from to ocean to the atmosphere. Precipitation is return of water to the ocean from the atmosphere in form of rain and snow.

Significance

Water is the essential element for life. Over 70% of the Earth's surface is covered by the ocean, which forms the largest reservoir of water on earth. The never-ending recycling process in which a small fraction of water is continuously removed from the ocean as excess evaporation over precipitation into the atmosphere, redistributed through atmospheric circulation, deposited as excess precipitation over evaporation on land, and returned to the ocean as river discharge, is critical to the existence of human life and the variability of weather and climate.

With their high specific heat and large thermal inertia, the oceans are also the largest reservoir of heat and the flywheel of the global heat engine. Since water has high latent heat, evaporation is also an efficient way to transfer the energy. Besides releasing latent heat to the atmosphere, the water transported from the ocean to the atmosphere forms clouds, which absorb and reflect radiation. Water vapor is also an important greenhouse gas, which absorbs more long-wave radiation emitted by Earth than the short-wave radiation from the Sun. Redistribution of clouds and water vapor changes the Earth's radiation balance.

The differential heating of the atmosphere by the ocean fuels atmospheric circulation, which, in turn, drives ocean currents. Both wind and current transport and redistribute heat and greenhouse gases. Adding heat and water changes density of air and seawater. The heat and water fluxes, therefore, change both the baroclinicity and stability (horizontal and vertical density gradients) of the atmosphere and the ocean. These, in turn, modify the shears of wind and current.

Spacebased Estimation

The equation of water balance in the atmospheric column is

$$\frac{\partial W}{\partial t} + \nabla \cdot \boldsymbol{\Theta} = E - P = F \qquad (1)$$

where

$$\Theta = \int_0^{p_s} q\mathbf{u}dp \qquad (2)$$

is the moisture transport integrated over the depth of the atmosphere, and

$$W = \frac{1}{g}\int_0^{p_s} q\,dp \qquad (3)$$

is the precipitable water, or column integrated water vapor. In these equations, p is the pressure, p_s is the pressure at the surface, q and **u** are the specific humidity and wind vector at a certain level. Bold symbols represent vector quantities. F is the fresh water exchange between the ocean and the atmosphere and is the difference between evaporation (E) and precipitation (P) at the surface. The first term is the change of storage. For periods longer than a few days, it is negligible, and there is a balance between the divergence of the transport ($\nabla\cdot\boldsymbol{\Theta}$) and the surface flux. The balance gives rise to two ways of estimating the fresh water flux. One is to measure E and P separately; the other is to estimate $\boldsymbol{\Theta}$. There are many programs to produce P (see Rainfall, by R. Ferraro, in this book) and we will not discuss it in this paper. One of the most advanced statistical techniques, support vector regression (SVR) has been used recently to retrieve surface specific humidity (q_s), E, and $\boldsymbol{\Theta}$, from spacebased data.

E is air-sea exchange of water vapor by turbulence; the small-scale turbulence is largely independent of factors governing large-scale atmospheric circulation (e.g., baroclinicity, Coriolis force, pressure gradient force, cloud entrainment), while $\boldsymbol{\Theta}$ is not as sensitive as E to small-scale ocean processes. Meteorologists sometimes view the traditional way of estimating E through the small turbulent-scale processes as the "supply side" estimation; the water is supplied by the ocean. The large-scale atmospheric divergence demands the water flux from the ocean and the estimation of E from $\nabla\cdot\boldsymbol{\Theta}$ is termed as the "demand side" estimation.

Bulk Parameterization-the supply side

Most productions of spacebased evaporation data sets in the past were based on bulk parameterization.. Latent heat flux (LH) is related to E by the nearly constant value of latent heat of vaporization(L): LH=L×E. LH, rather than E, is used in many of the past studies. The two parameters are used interchangeably in this paper, and our discussion on E applies equally to LH.

The computation of E by the bulk parameterization requires sea surface temperature (SST), wind speed (u), and q.

$$E = C_E \rho u (q_s - q) \qquad (4)$$

where C_E is the transfer coefficient, □ is the surface air density. q_s is usually taken to be the saturation humidity at SST multiplied by a factor of 0.98 to account for the effect of salt in the water. u and q should be measured in the atmospheric surface (constant flux) layer, usually taken at a reference level of 10 m. Over the ocean, u and SST have been measured from space, but not q. A method of estimating E using satellite data was demonstrated by Liu and Niiler (1984), based on an empirical relation between W and q on a monthly time scale over the global ocean (Liu 1986). The physical rationale is that the vertical distribution of water vapor through the whole depth of the atmosphere is coherent for periods longer than a week (Liu et al. 1991). The relation has been scrutinized in a number of studies and many variations of this method have been

proposed to improve on the estimation (see Liu and Katsaros, 2001, for a review of earlier studies). Modification of this method by including additional estimators has been proposed (e.g., Wagner et al. 1990; Cresswell et al. 1991; Miller and Katsaros 1991; Chou et al. 1995), with various degrees of improvement. Recently, neural network has also been used to mitigate the non-linearity problem in derive q (Jones et al. 1999; Bourras et al. 2002; Roberts et al. 2010). Algorithms to retrieval q from brightness temperatures (BT) measured by microwave radiometers were developed and improvements were demonstrated (e.g., Schultz et al. 1997; Schlüssel et al. 1995; Jackson et al. 2009). Yu and Weller (2007) have combined spacebased observations with model output. Fig. 1 shows the validation of q derived from BT measured by the Advanced Microwave Scanning Radiometer - Earth Observing System (AMSR-E) through a statistical model built on SVR. The model outputs are compared with coincident q measured at buoys. For the year of 2008, 30,000 buoy data were randomly selected for validation. The mean and root-mean-square (rms) differences are 0.05 and 1.05 g/kg respectively. The rms difference is only 5% of the range of 20 g/kg and the statistical model appears to be successful. However, E depends on $\Delta q=q_s-q$, which is the small difference between the two large terms (q_s and q), and a small percentage error in q may still cause a large error in Δq and E.

Liu (1990) suggested and demonstrated two potential ways to improve E retrieval from satellite data. The first is to incorporate information on vertical distribution of humidity given by atmospheric sounders. Jackson et al. (2009) have recently adopted this suggestion. The other is to retrieve E directly from the radiances, since all the bulk parameters used in the traditional method could be derived from radiances measured by a microwave radiometer. The direct retrieval method may improve accuracy in two ways. The first is to by-pass the uncertainties of the bulk transfer coefficients to be used. The second is to mitigate the magnification of error caused by multiplying inaccurate measurement of wind speed with inaccurate measurements of humidity (q and q_s) in the bulk formula.

Fig. 2 compares the uncertainties of two sets of LH derived from the two methods. For the first set, SST and u from AMSR-E produced by Remote Sensing System (Wentz and Meissner, 2000) are used with q derived from AMSR BT (same as those in Fig. 1). The second set is the output of a statistical model built on SVR, predicting E from the 12-channel AMSR-E BT. A total of 30,000 randomly selected LH computed from 3 groups of buoy data in 2008 are used in the validation exercise. Direct retrieval of daily values reduces the rms difference from 77 w/m2 of the bulk parameterization method to 38 w/m2. This is equivalent to a reduction from 19% to 9.7% of the dynamic range of 400 W/m2.

The available E (or LH) products and the bulk parameters used to derive them exhibit substantial differences (e.g., Brunke et al. 2002; Bourras 2006; Smith et al. 2011; Santorelli et al., 2011). The conservation principle (Eq. 1) and the demand side evaluation may serve as an effective way to evaluate current E products.

Divergence of Moisture Transport-the Demand Side

The computation of $\boldsymbol{\Theta}$, as defined in Eq. 2, requires the vertical profile of q and **u**, which are not measured by spacebased sensors with sufficient resolution. $\boldsymbol{\Theta}$ can be viewed as the column of water vapor W advected by an effective velocity $\mathbf{u_e}$, so that $\mathbf{u_e}=\boldsymbol{\Theta}$/W, and $\mathbf{u_e}$ is the depth-averaged wind velocity weighted by humidity. W has been derived from microwave radiometer measurements with good accuracy. Methods were developed to related $\mathbf{u_e}$ to the equivalent neutral wind measured by scatterometers, $\mathbf{u_s}$, based on polynomial regression (Liu 1993) and neural network (Liu and Tang 2005). Xie et al. (2008) added cloud-drift winds at 850 mb to $\mathbf{u_s}$, and used SVR instead of neural network. The scatterometer measurement and the cloud drift winds represent ocean surface stress and free-stream velocity respectively. Xie et al. (2008) show the $\boldsymbol{\Theta}$ derived from their statistical model agree with $\boldsymbol{\Theta}$ derived from 90 rawinsonde stations from synoptic to seasonal time scales and from equatorial to polar oceans. Hilburn (2010) found very good agreement between this data set and data computed from Modern Era Retrospective-analysis for Research and Applications (MERRA) over the global ocean. MERRA is a NASA atmospheric reanalysis using a major new version of the Goddard Earth System Data Assimilation System (Rienecker et al. 2011). Fig. 2 shows that, for a total of 26,000 pairs randomly selected data, 2/3 from rawinsonde and 1/3 from the reanalysis, the RMS difference is 57.5 kg/m/s and the correlation coefficient is 0.95 for zonal component, and 49.7 kg/m/s and 0.89 for meridional component, for a range of approximately -600 to +600 kg/m/s.

Validation of our spacebased estimation of $\nabla\cdot\boldsymbol{\Theta}$ as F was achieved through mass balance over ocean and continent, using the Gravity Recovery and Climate Experiment (GRACE), which is a geodesy mission to measure Earth's gravity field. The variations of the gravity field are largely the results of the change of water storage. The air-sea water flux given by $\nabla\cdot\boldsymbol{\Theta}$ integrated over all ocean area, together with river discharge (R) from all continents should balance the rate of mass change (∂M/∂t) of all oceans:

$$\iint \frac{\partial M}{\partial t} = \int R - \iint \nabla\cdot\Theta \qquad (5)$$

Fig. 3 shows that monthly rate of mass change (-∂M/∂t), measured by GRACE, integrated over all oceans, balances $\nabla\cdot\boldsymbol{\Theta}$ (Xie et al. 2008) integrated over the ocean areas minus the line-integral of R over all coastlines, both in magnitude and in phase. The difference between -$\iint\partial$M/∂t and $\iint\nabla\cdot\boldsymbol{\Theta}$-$\int$R has a mean of 2.1 10^8kg/**s** and a standard deviation of 2.6 10^8kg/**s**, for a peak-to-peak variation of more than 10 10^8kg/s. The uncertainties in time varying river discharge and ice melt contribute to a large part of error. Mass is conserved in the long term, and first term in Eq. 5 is negligible. The total ocean surface water flux should balance the total water discharge from continent to ocean. The $\iint\nabla\cdot\boldsymbol{\Theta}$ four-year mean of 10.6 cm/yr, computed from outputs of the statistical model is lower than the climatological value of 12 cm/yr given in text book published 36 years ago (Budyko 1974), and higher than the climatological river discharge of 8.6 cm/yr (Dai and Trenberth 2002). There are, in general, 20% uncertainties of these hydrologic parameters over global ocean.

Based on Green's Theorem, the areal integral of the flux divergence should balance the line integral of flux out of the area. The last term of Eq. 5 should equal to total water

vapor across the coastlines of all continents. Another example of the role of Θ in the conservation principle is given by Liu et al. (2006). They showed that across the entire coastline of South America, with the river discharge removed, agrees with the mass change of the continent both in magnitude and phase of seasonal changes.

Comparison Between Supply and Demand

As an example, the three-year averages of $\nabla\cdot\Theta$ and E-P are shown in Figure 5. In this example, P is based on Tropical Rain Measuring Mission (TRMM) Microwave Imager product, and E is from our direct retrieval from BT. There are general agreement is the magnitude and geographical distribution, but differences in the details. Away from coastal regions, the supply side is larger than the demand side in the tropical southeastern Pacific, tropical south Atlantic, and a region from the Somali coast extending into the northern Arabian Sea. The demand side is larger than the supply side in the warm pool of the western tropical Pacific and under the ITCZ. The differences may reveal regional hydrodynamics.

Summary

There have been continuous endeavors to estimate E and LH over global oceans using satellite data and based on bulk parameterization of turbulence transport, since Liu and Niiler (1984) successfully estimated the flux by introducing an empirical relation between monthly W and q. With some improvement in this 'supply side' approach, a number of data sets have been operationally produced in the past two decades, but large differences among these data sets and between products from satellite data and from re-analysis of operational weather prediction remain (e.g. Curry et al. 2004). Evaluations to find the optimal product are difficult because of the lack of credible standards (e.g., extensive direct flux measurement). One good constraint to the uncertainties is the closure of the atmospheric water budget, which dictates that E-P should balance $\nabla\cdot\Theta$. The 'demand side' approach of estimating Θ and $\nabla\cdot\Theta$ from satellite data serves not only as a credible way to evaluate traditional 'supply side' flux products but also to provide the ocean fresh water exchange as a whole, without securing precipitation separately. The Θ data have been extensively tested in comparison with all available rawinsonde data and products of numerical models. The water flux data, as $\nabla\cdot\Theta$, are also validated through mass conservation using gravity data from GRACE and river discharge, to within 20% of the seasonal cycle. We have also introduced a new method of direct retrieval of E and LH from the measured radiances, which improves the random error of the daily value of LH to 10% of the dynamic range from 19% error for computing the fluxes from bulk parameters derived from the same radiances. There is still much room left for improvement. The new spacebased data products, with better spatial and temporal resolution, have many ongoing scientific applications.
.

Acknowledgment

This report was prepared at the Jet Propulsion Laboratory (JPL), California Institute of Technology, under contract with the National Aeronautics and Space Administration (NASA). The Precipitation Measuring Mission, Physical Oceanography Program and the Aquarius Science Team of NASA jointly supported this effort. The Climate Science Center of JPL supported the data production in its strategic planning.

References

Bourras, D., L. Eymard, and W.T. Liu, 2002: A neural network to estimate the latent heat flux over oceans from satellite observations. Int. J. Remote Sens., 23, 2405-2423.

Bourras, D., 2006: Comparison of five satellite-derived latent heat flux products to moored buoy data. J. Clim., 19, 6291-6313.

Brunke, M.A., X. Zeng, and S. Anderson, 2002: Uncertainties in sea surface turbulent flux algorithms and data sets. J. Geophys. Res., 107(C10), 3141, doi:10.1029/2001JC000992.

Budyko, M. I., 1974: Climate and life, Academic, New York.

Chou, S.H., R.M. Atlas, and J. Ardizzone, 1995: Estimates of surface humidity and latent heat fluxes over oceans from SSM/I data. Mon. Wea. Rev., 123, 2405-2435.

Cresswell, S., E. Ruprecht, and C. Simmer, 1991: Latent heat flux over the North Atlantic Ocean-A case study. J. Appl. Meteor., 30, 1627-1635.

Curry, J.A. and 22 others, 2004: Seaflux. Bull. Amer. Meteor. Soc., 85, 409-419.

Dai, A., and K. E. Trenberth, 2002: Estimates of freshwater discharge from continents: Latitudinal and seasonal variations. J. Hydrometeorol., 3, 660-687.

Hilburn, Kyle A., 2010, Intercomparison of water vapor transport datasets, presented at 17th Conference on Satellite Meteorology and Oceanography and 17th Conference on Air-Sea Interaction, Annapolis, MD.

Jackson, D. L., G. A. Wick, and F. R. Robinson, 2009: Improved multisensor approach to satellite-retrieved near-surface specific humidity observations. J. Geophys. Res., 114, D16303. doi:10.1029/2008JD011341.

Jones, C., P. Peterson, and C. Gautier, 1999: A new method for deriving ocean surface specific humidity and air temperature: An artificial neural network approach. J. Appl. Meteorol., 38, 1229-1245.

Liu, W.T., and P.P. Niiler, 1984: Determination of monthly mean humidity in the atmospheric surface layer over oceans from satellite data. J. Phys. Oceanogr., 14, 1451-1457.

Liu, W.T., 1986: Statistical relation between monthly precipitable water and surface-level humidity over global oceans, Mon. Wea. Rev., 114, 1591-1602.

Liu, W.T., 1990: Remote Sensing of surface turbulence flux. Surface Waves and Fluxes,Vol. II,. G.L. Geenaert and W.J. Plant (eds), Kluwer Academic, Chapter 16, 293-309.

Liu, W.T., W. Tang and P.P. Niiler, 1991: Humidity Profiles Over Ocean. J. Climate, 4, 1023-1034.

Liu, W. T., 1993: Ocean Surface Evaporation. Atlas of Satellite Observations Related to Global Change, R.J. Gurney, J. Foster, and C. Parkinson (eds.), Cambridge University Press, Cambridge, 265-278.

Liu, W.T., and K.B. Katsaros, 2001: Air-Sea Flux from Satellite Data. Ocean Circulation and Climate. G. Siedler. J. Church, and J. Gould (eds), Ch. 3.4, 173-1179, Academic Press, New York.

Liu, W.T., and W. Tang, 2005: Estimating moisture transport over ocean using spacebased observations from space. J. Geophys. Res., 110, D10101, doi:10.1029/2004JD005300.

Liu, W. T., X. Xie, W. Tang, and V. Zlotnicki, 2006: Spacebased observations of oceanic influence on the annual variation of South American water balance. Geophys. Res. Lett., 33, L08710, doi:10.1029/2006GL025683.

Miller, D.K., and K.B. Katsaros, 1991: Satellite-derived surface latent heat fluxes in a rapidly intensifying marine cyclone. Mon. Wea. Rev., 120, 1093-1107.

Rienecker, M. M., and Coauthors, 2011: MERRA: NASA's Modern-Era Retrospective Analysis for Research and Applications. J. Clim., 24, 3624–3648.

Roberts, B., C. A. Clayson, F. R. Robertson, D. Jackson, 2010: Predicting near-surface atmospheric variables from SSM/I using neural networks with a first guess approach. J. Geophys. Res., submitted.

Santorelli1, A., R. T. Pinker, A. Bentamy, K. B. Katsaros, W. M. Drennan, A. M. Mestas-Nuñez, and J. A. Carton: Differences between two estimates of air-sea turbulent heat fluxes over the Atlantic Ocean. J. Geophys. Res., 116, C09028, doi:10.1029/2010JC006927.

Schlüssel, P., L. Schanz, and G. Englisch, 1995: Retrieval of latent heat flux and longwave irradiance at the sea surface from SSM/I and AVHRR measurements. Adv. Space Res., 16, 107 – 116, doi:10.1016/0273-1177(95)00389-V.

Schulz, Jörg, Jens Meywerk, Stefan Ewald, and Peter Schlüssel, 1997: Evaluation of satellite-derived latent heat fluxes. J. Climate, 10, 2782–2795.

Smith, S.R., P. J. Hughes and M. A. Bourassa: 2011: A comparison of nine monthly air-sea flux product. Int. J. Climatol., 3, 1002-1027. DOI: 10.1002/joc.2225.

Wagner, D., E. Ruprecht, and C. Simmer, 1990: A combination of microwave observations from satellite and an EOF analysis to retrieve vertical humidity profiles over the ocean. J. Appl. Meteor., 29, 1142-1157.

Wentz, F.J., and T. Meissner, 2000: AMSR Ocean Algorithm, Version 2, report number 121599A-1, Remote Sensing Systems, Santa Rosa, CA, 66 pp.

Xie X., W.T. Liu, and B. Tang, 2008: Spacebased estimation of moisture transport in marine atmosphere using support vector machine. Remote Sens. Environment, 112, 1846-1855.

Yu, L., and R. A. Weller, 2007: Objectively Analyzed air-sea heat Fluxes (OAFlux) for the global ice-free oceans. Bull. Amer. Meteor. Soc. 88, 527-539.

List of Figures

Fig. 1 Bin-average of near surface specific humidity (q) derived from the statistical model compared with values measured at three groups of buoys. Standard deviation is superimposed on each bin average as error bar.

Fig. 2 Bin-average of latent heat flux (LH) derived directly from the satellite measured radiances (a), and computed from bulk parameters (b), compared with coincident

measurements at three groups of buoys. Standard deviation is superimposed on each bin average as error bar.

Fig. 3 Bin-averaged zonal component (a) and meridional component (b) of integrated moisture transport (**Θ**). derived from satellite data, compared with co-incident data computed from rawinsondes.

Fig. 4 Annual variation of hydrologic parameters integrated over global oceans.

Fig. 5 Three year (2003-2005) annual mean distribution of (a) the divergence of integrated moisture transport, and (b) evaporation-precipitation derived from AMSR-E and TMI.

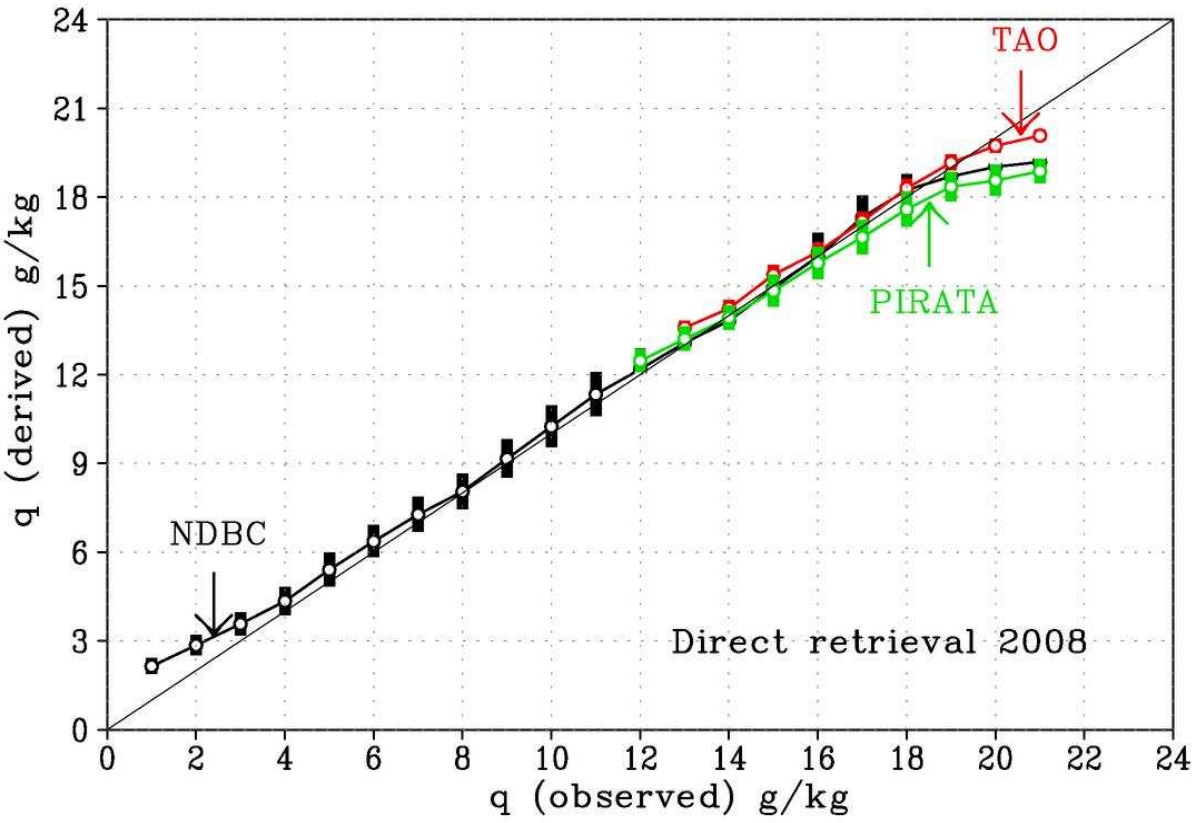

Fig. 1 Bin-average of near surface specific humidity (q) derived from the statistical model compared with values measured at three groups of buoys. Standard deviation is superimposed on each bin average as error bars.

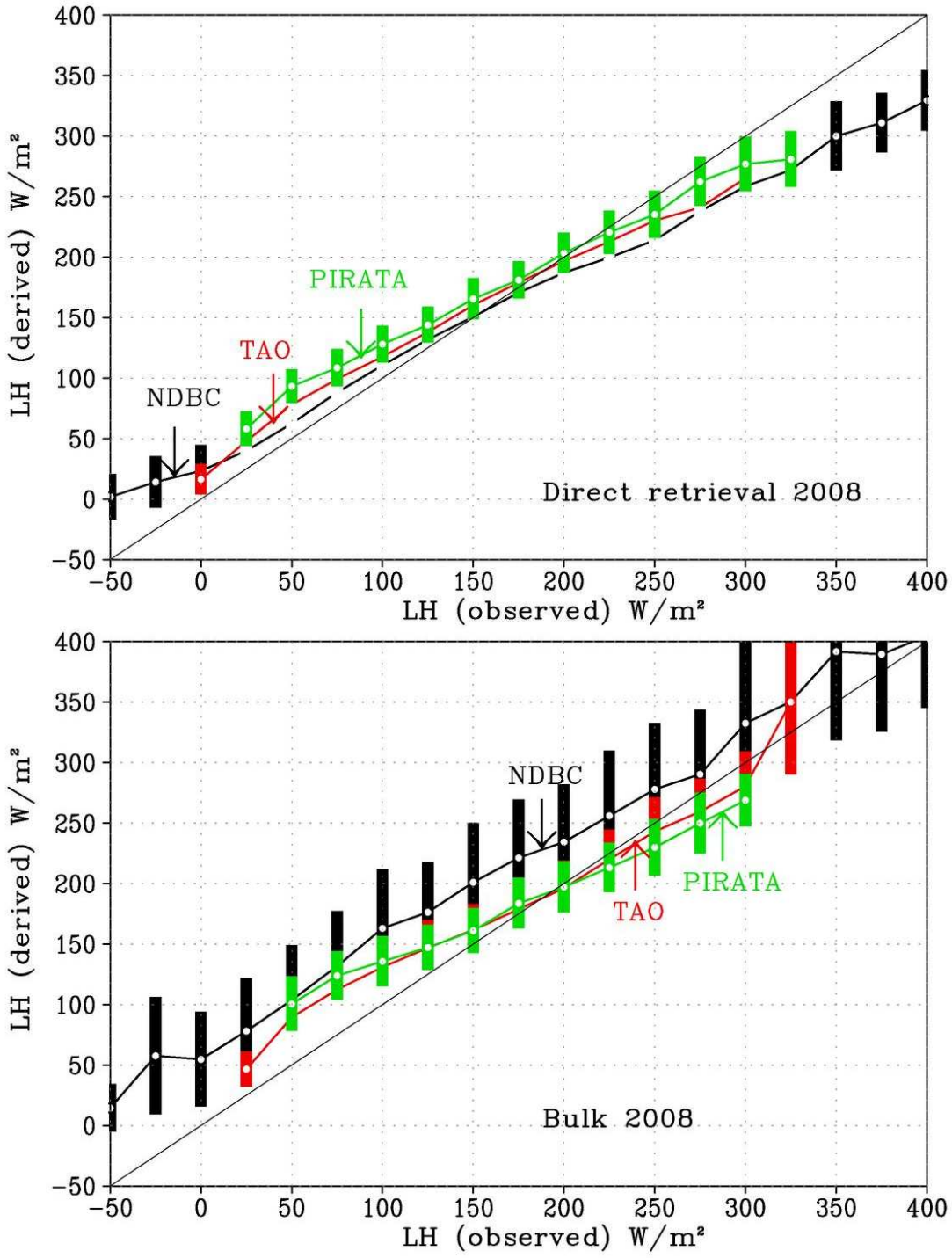

Fig. 2 Bin-average of LH derived directly from the satellite measured radiance (a) compared with values computed from bulk parameters (b) measured at three groups of buoys. Standard deviation is superimposed on each bin average as error bars.

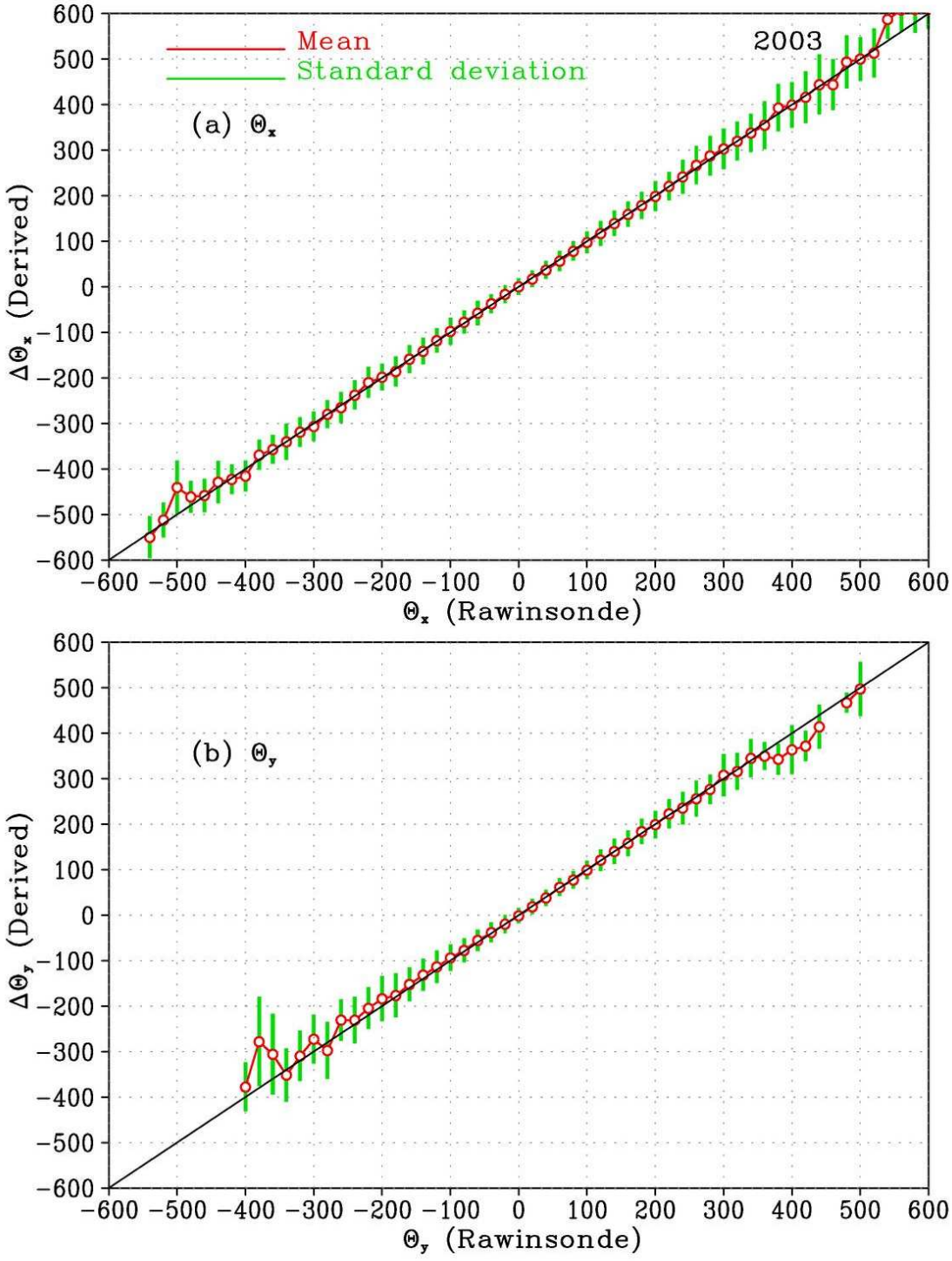

Fig. 3 Bin-averaged zonal component (a) and meridional component (b) of integrated moisture transport (**Θ)**, derived from satellite data, as compared with co-incident data computed from rawinsondes. Standard deviation is superimposed on each bin average as error bars.

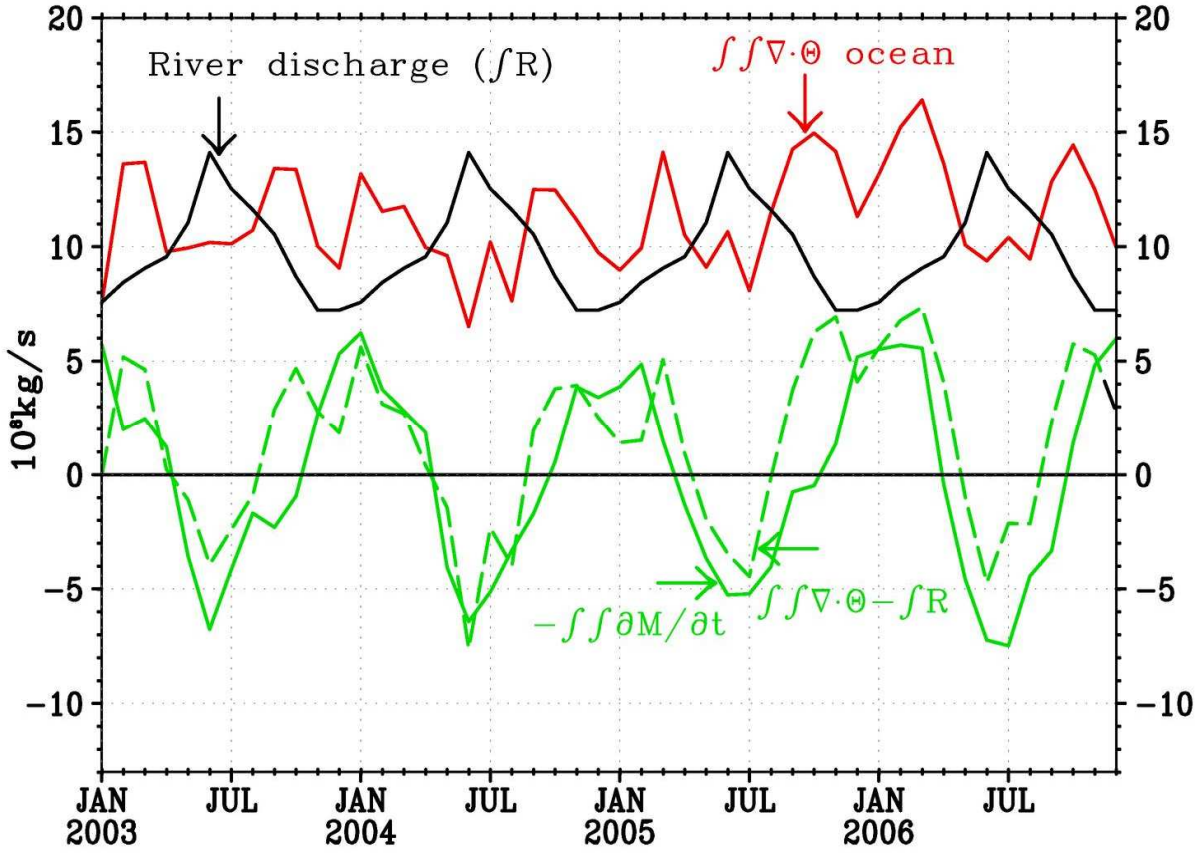

Fig. 4 Annual variation of hydrologic parameters integrated over global oceans.

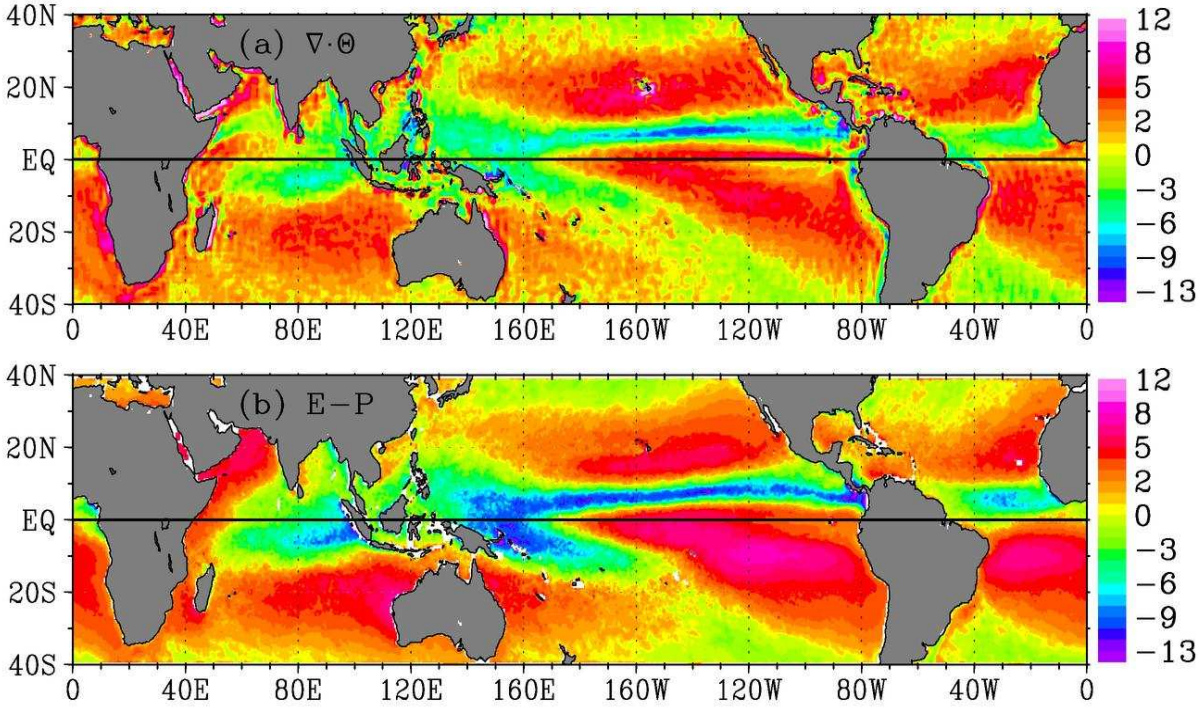

Fig. 5 Annual mean distribution of the divergence of three years between 2003-2005 (a), and evaporation-precipitation, derived from AMSR-E and TMI respectively (b).